Songklanakarin J. Sci. Technol.
31 (5), 463-470, Sep. - Oct. 2009

Songklanakarin Journal
of Science and Technology
http://www.sjst.psu.ac.th

Invited Paper

Two stage S-N curve in corrosion fatigue of extruded magnesium alloy AZ31

M.S. Shahnewaz Bhuiyan[1] and Yoshiharu Mutoh[2]

[1] *Department of Materials Science,*

[2] *Department of System Safety,*
Nagaoka University of Technology, 1603-1 Kamitomioka, Nagaoka-shi, Niigata 940-2188, Japan

Abstract

Tension-compression fatigue tests of extruded AZ31 magnesium alloys were carried out under corrosive environments: (a) high humidity environment (80 %RH) and (b) 5 wt. %NaCl environment. It was found that the reduction rate of fatigue strength due to corrosive environment was 0.12 under a high humidity and 0.53 under a NaCl environment. It was also observed that under corrosive environments, the S-N curve was not a single curve but a two-stage curve. Above the fatigue limit under low humidity, the crack nucleation mechanism was due to a localized slip band formation mechanism. Below the fatigue limit under low humidity, the reduction in fatigue strength was attributed to the corrosion pit formation and growth to the critical size for fatigue crack nucleation under the combined effect of cyclic load and the corrosive environment. The critical size was attained when the stress intensity factor range reached the threshold value for crack growth.

Keywords: fatigue, corrosion fatigue, two stage S-N curve, corrosion pit, humidity, NaCl, magnesium alloy.

1. Introduction

Magnesium alloys are known as very light structural materials with excellent physical and mechanical properties, such as low-density, high specific strength, good damping characteristics, good electromagnetic shielding characteristics, good machinability, and recyclability. These properties make magnesium alloys valuable in industrial applications including automotive components, computer parts, aerospace components and cellular phone parts, where weight reduction is of great concern (Friedrich *et al.*, 2001; Mordike *et al.*, 2001;Gray *et al.*, 2002; Lua, 2002; Arruebarrena *et al.*, 2005; Abbas *et al.*, 2005; Rosalbino *et al.*, 2005; Kulekcri, 2008;). However, magnesium and its alloys are characterized by low corrosion resistance, which makes their use limited (Makar *et al.*, 1990; Song *et al.*, 1999, Ambat *et al.*, 2000;). In order to apply magnesium alloys to high strength structural components in automobile, aerospace and other transportation industries, the characterization of fatigue properties, especially under corrosive environments, is highly required.

Research works on fatigue of various structural materials conducted throughout the last half century have clearly indicated that the presence of aggressive environment drastically reduces the components' life time (Gough, 1932; McAdam *et al.*, 1941; Wescott, 1938). This provides a strong warning to design engineers to take corrosion fatigue into account in designing components and structures subjected to fatigue loading in a corrosive environment. Fatigue loads and corrosive environment are two independent agents that cause strength degradation in structural materials (Davis, 1998; Schijve, 2003). Numerous experimental investigations have shown that corrosion fatigue cracks start from corrosion pits (Uhlig *et al.*, 1971; Magnin *et al.*, 1989), even at very low stress amplitudes. These research works have been carried out on steels, aluminum alloys and other materials.

However, only few research works related to corrosion fatigue behavior of magnesium alloys have been carried out. Hilpert and Wagner (Hilpert, 2000) examined the fatigue behavior of extruded high strength AZ80 magnesium alloy

*Corresponding author.
Email address: newaz@stn.nagaokaut.ac.jp,
mutoh@mech.nagaokaut.ac.jp

Table 1. Chemical composition of the AZ31 alloy used (mass %)

Al	Zn	Mn	Fe	Si	Cu	Ni	Mg
3.15	0.79	0.28	0.004	0.020	0.0024	0.0008	Bal

Table 2. Mechanical properties of the AZ31 alloy used

Yield stress (MPa)	Tensile strength (MPa)	Elongation (%)	Young's Modulus (GPa)
206	242	22.62	48

under spraying of aqueous NaCl solution. The fatigue life was considerably reduced at stresses below the fatigue limit under ambient air, while no significant effect of NaCl solution on fatigue life was found at higher stress amplitudes. Unigovski et al. (Unigovski, 2003) carried out the corrosion fatigue tests of extruded AZ31, AZ91D and die cast AM50 magnesium alloys under an aggressive environment and reported that extruded alloys showed a significantly longer fatigue life in both air and NaCl solution in comparison with the die-cast alloy, which suggests that the influence of casting defects is more dominant compared to the influence of a corrosive environment. Z. B. Sajuri *et al.* (Sajuri *et al.*, 2005) studied the fatigue behavior of extruded AZ61 magnesium alloy under tension-compression loading and reported that corrosion pits were formed in the early stage of the fatigue process under high humidity, which enhanced early fatigue crack nucleation at lower stress amplitudes.

The authors (Bhuiyan *et al.*, 2008) investigated the corrosion fatigue behavior of extruded AZ61 magnesium alloy under (a) high humidity (80 % relative humidity (RH)), (b) sprayed 5 wt% NaCl solution environment, and (c) sprayed 5 wt% $CaCl_2$ solution environment. They found that fatigue strength was drastically reduced under the three different corrosive environments: the reduction rates of fatigue limit under high humidity, NaCl and $CaCl_2$ environments were 0.22, 0.85 and 0.77, respectively. The drastic reduction in fatigue limit under corrosive environments resulted from pit formation and growth to the critical size for fatigue crack nucleation. It was suggested that the NaCl environment enhances the pit formation and growth more than the $CaCl_2$ environment, due to the high Cl^- concentration and low the pH value. As mentioned above, detailed investigation on corrosion fatigue of AZ61 alloy were available. However, for the AZ31 alloy with lower strength and higher ductility, only two reports on corrosion fatigue were available (Hilpert *et al.*, 2000; Unigovski *et al.*, 2003), but a detailed investigation especially on the corrosion pit formation mechanism under NaCl environment has not yet been carried out. Therefore, it is of importance to understand the detailed corrosion fatigue characteristics of AZ31 alloy for its practical application.

In the present study, for understanding the basic corrosion fatigue behavior of AZ31 alloy, fatigue tests of extruded AZ31 alloy were conducted under low humidity, high humidity (80 % relative humidity (RH)), and sprayed 5 wt% NaCl solution environments.

2. Material and Experimental Procedures

The material used in the present study was an extruded AZ31 magnesium alloy. Chemical composition and mechanical properties of the AZ31 alloy used are shown in Tables 1 and 2, respectively. Microstructure of the as-received 16 mm diameter extruded AZ31 alloy bar were observed under a digital microscope, where equi-axed grains and no deformation twins were observed as shown in Figure 1. Somekawa *et al.* (Somekawa *et al.*, 2007) also reported similar microstructures of extruded AZ31 magnesium alloy.

Round bar fatigue specimens with threaded end were used; shape and dimensions of which are indicated in Figure 2. After machining, the specimens were polished in the loading direction with 280 to 800 grit emery papers in laboratory air and with 1000 to 1500 grit emery papers under kerosene oil to prevent corrosion of the specimen surface during the polishing process. After all polishing processes were completed the specimens were cleaned by ethanol in an ultrasonic cleaner.

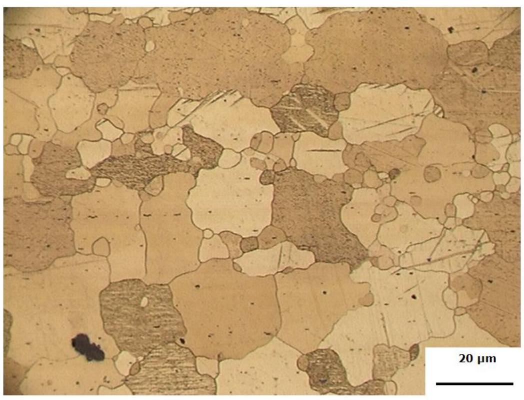

Figure 1. Microstructure of the AZ31 magnesium alloy.

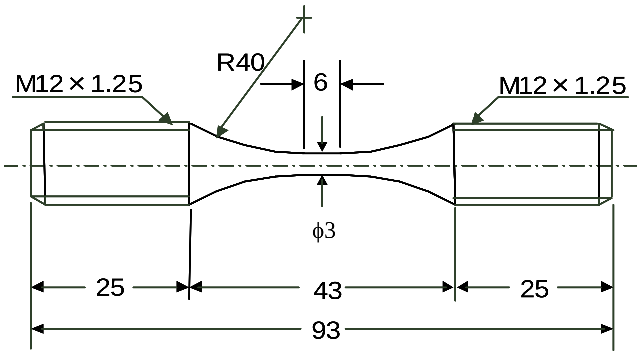

Figure 2. Shape and Sizes of the fatigue specimen.

Fatigue tests were conducted on a servo-hydraulic fatigue testing machine using a sinusoidal wave form with a frequency of 20 Hz and a stress ratio of -1 under two corrosive environments: (a) high humidity environment (80% RH) and (b) sprayed 5 wt% NaCl solution environment with a pH value of 6.59 (noted as NaCl environment). Fatigue tests under high humidity (80% RH) were conducted in a specially designed chamber which can control the relative humidity level ranging from 30 to 80 % RH. Fatigue tests under the NaCl environment was conducted in a 31.5×26.5×17 c m chamber by spraying the solution with a flow volume of 1.6 ml/h at 0.1 MPa air pressure, where the temperature of solution was 25.1°C and the temperature inside the chamber was 25.4°C. The fatigue test was continued up to complete failure of the specimen, while the test was stopped when the specimen did not fail up to 10^7 cycles. The fatigue tests for obtaining the basic fatigue properties of AZ31 alloy without corrosion effect were also carried out at 16°C -20°C under low humidity of 35-40 % RH.

Specimen surfaces and fracture surfaces were observed in detail by using a scanning electron microscope (SEM) to investigate the pitting process and the fracture surface morphology under the three different environments.

3. Results and Discussion

3.1 S-N curves

S-N curves under three different environments are shown in Figure 3. The subscript "P" in the figure indicates that fatigue crack started from a corrosion pit. As can be seen from the figure, the present AZ31 alloy shows a fatigue limit of about 88 MPa under low humidity environment without corrosion effect. However, the fatigue strength at 10^7 cycles was significantly reduced to 75 MPa and 40 MPa under high humidity environment and NaCl environment, respectively.

The effect of corrosive environment on the fatigue strength is evaluated by using the reduction rate of fatigue limit (RRFL), which is given as:

$$RRFL = \frac{\sigma_{LH} - \sigma_{CE}}{\sigma_{LH}} \times 100\% \quad (1)$$

where σ_{LH} is the fatigue limit under low humidity condition and σ_{CE} is that under corrosive environment.

The evaluated values under corrosive environments for the present materials are shown in Table 3. It can be seen from the table that the NaCl environment reduces the fatigue limit 3.7 times more than the high humidity (80% RH) environment. By using Equation 1, similar results have been obtained on several magnesium alloys, which are listed in Table 3. From the data, it seemed that the fatigue strength under the NaCl environment of higher strength magnesium alloys (AZ80, AZ61) degraded more than those of lower strength magnesium alloys (AM50, AZ31), while the fatigue data for all the magnesium alloys under NaCl environment were in a wide range of RRFL values (27% to 87%).

As can be seen from Figure 3, an important finding is that, the S-N curves under corrosive environments showed a two stage curve. In the first stage (above the stress amplitude of 90 MPa), the crack nucleation mechanism would be due to the localized slip band formation mechanisms, which is common in various metals under a non-corrosive environment. In this stage the applied stress can provide a sufficient mechanical driving force to produce slip bands and the environmental effect cannot be attended. In the second stage (below the stress amplitude of 90 MPa), the reduction in fatigue strength is caused by corrosion pit formation due to the combined effect of cyclic loading and the corrosive environment (Sajuri *et al.*, 2005). Therefore, the two-stage S-N curve under corrosive environment would be induced by the difference of the crack nucleation mechanism between the two stages.

Similar two stage S-N curves are well known for high strength steels as "ultra-high-cycle fatigue", which results from two different crack nucleation mechanisms(Asami *et al.*, 1985; Euromech Colloquium 382, 1999). In the high cycle fatigue region at higher cyclic stresses, the fatigue crack nucleation is induced by the localized slip bands formation mechanism on the specimen surface, while a fatigue crack

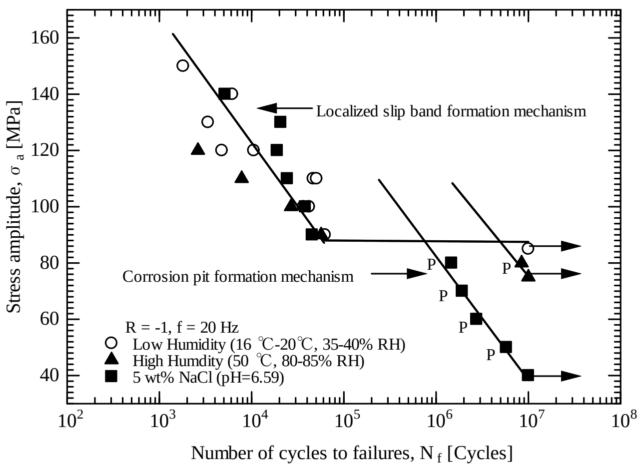

Figure 3. S-N curves for extruded AZ31 magnesium alloy under corrosive environments.

Table 3. Effect of corrosive environment on fatigue limit of magnesium alloys

Material	Test Environment	Test conditions	RRFL $\frac{(\sigma_{LH} - \sigma_{CE})}{\sigma_{LH}}$	Ref.
Extruded AZ80	Sprayed 3.5% NaCl solution	f = 60 R = -1	0.73	Hilpert *et al.*, 2000
Electro polishedAZ80	3.5% NaCl solution	f = 60 R = -1	0.80	Hilpert *et al.*, 2000
Extruded AZ61	High humidity (80%)	f = 10 R = -1	0.27	Sajuri *et al.*, 2005
Extruded AZ61	High humidity (80%)	f = 20	0.22	Bhuiyan *et al.*, 2008
	Sprayed 5% NaCl	R = -1	0.87	
Extruded AM50	3.5% NaCl solution	f = 30 R = -1	0.27	Unigovski *et al.*, 2003
Extruded AZ31	3.5% NaCl solution	f = 30 R = -1	0.34	Unigovski *et al.*, 2003
Electro polished AZ31	3.5% NaCl solution	f = 60 R = -1	0.27	Helpert *et al.*, 2000
Extruded AZ31	High humidity (80% RH)	f = 20	0.15	Present work
	Sprayed 5% Nacl solution	R = -1	0.55	

σ_{LH} = Fatigue limit under low humidity, σ_{CE} = Fatigue limit under corrosive environment

nucleates from an inclusion inside the specimen in the ultra-high-cycle fatigue region at lower cyclic stresses.

3.2 Fracture surface observations

SEM fractographs for the specimen tested at stress level of 130 MPa under low humidity condition (36-40 % RH) are shown in Figure 4. The crack nucleation region is shown by a rectangular mark in Figure 4(a) and its high magnification is shown in Figure 4(b). The crack nucleation region showed that the crack nucleated from the surface of specimen without the existence of foreign particles such as inclusions and also defects on the specimen surface. The crack nucleation region was relatively flat with a transgranular fracture, which was commonly observed in smooth specimens of other structural metals.

Figure 5 shows SEM fractographs for the specimen tested under high humidity condition (80% RH) at stress amplitude of 120 MPa (higher than the fatigue limit under low humidity condition). The crack nucleation region revealed similar features that are found under low humidity conditions. However, under a high humidity environment, as the stress amplitude became lower than 88 MPa (the fatigue limit under low humidity condition) the failure of the specimen was attributed to the formation of a corrosion pit. Figure 6 shows the presence of a corrosion pit in the crack nuclea-

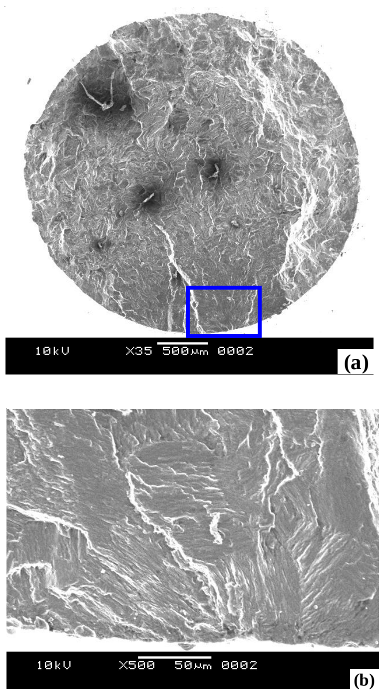

Figure 4. SEM fractographs showing (a) overall fracture surface, (b) magnified view of the crack nucleation region for the specimen tested at stress amplitude of 130 MPa under low humidity environment.

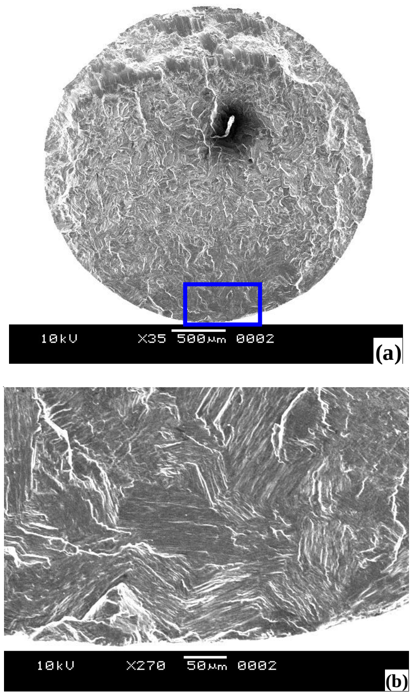

Figure 5. SEM fractographs showing (a) overall fracture surface, (b) magnified view of the crack nucleation region for the specimen tested at stress amplitude of 120 MPa.

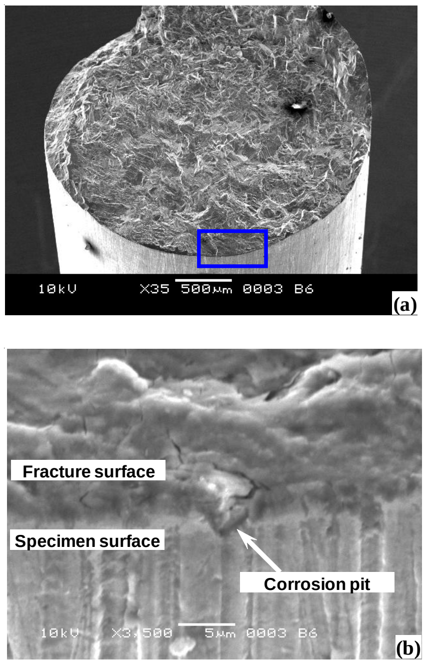

Figure 6. SEM fractographs showing (a) overall fracture surface, (b) corrosion pit at the crack initiation region for the specimen tested at stress amplitude of 80 MPa under high humidity environment.

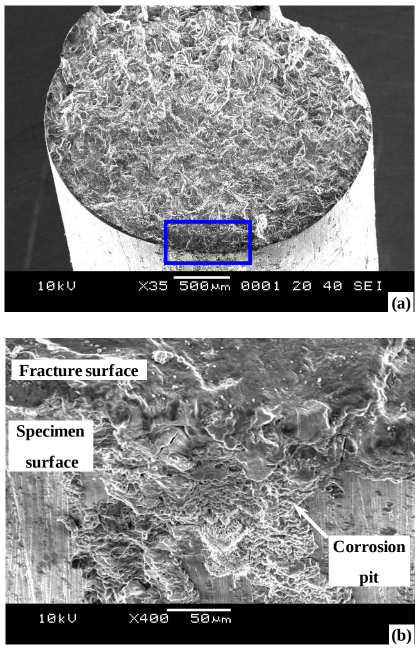

Figure 7. SEM fractographs showing (a) overall fracture surface, (b) corrosion pit at the crack initiation region for the specimen tested at stress amplitude of 80 MPa under the NaCl environment.

tion region on the specimen surface tested under high humidity condition (80% RH) at 80 MPa stress amplitude. Figure 7 shows fracture surfaces of the specimen tested under the NaCl environment at stress level of 80 MPa. A high magnification of the crack nucleation site revealed the existence of a corrosion pit. The significant reduction in fatigue strength under a corrosive environment can be also explained in terms of corrosion fatigue mechanism. It is known that the corrosion fatigue takes place in three stages, which is including pit formation, growth and crack nucleation from the pit and propagation (Dieter, 1976; Bayoumi, 1993). Corrosion pits are formed on the specimen surface in the early stage of fatigue life, and they act as stress concentrators causing crack nucleation and propagation (Forest, 1970; Pokhmurskii, 1983; Bayoumi, 1993) and are thus attributed to lower fatigue strength and shorter fatigue life.

3.3 Pit growth behavior under NaCl environment

The interrupted fatigue test at a stress amplitude of 50 MPa under the NaCl environment was carried out to investigate pit growth behavior under the NaCl environment. Figure 8 shows specimen surface observations for the specimen interrupted at various loading cycles. As can be seen from the figure, after 200,000 cycles (3.5% of total life), multiple corrosion pits were nucleated on the specimen surface (Figure 8(a)). The increase in the number of pits seemed to be significant higher than the increase in size of the pits with increasing number of cycles during fatigue loading under the NaCl environment. However, the formation sites of corrosion pits were not uniformly distributed but localized in some areas, as seen from Figure 8 (b). Coales-

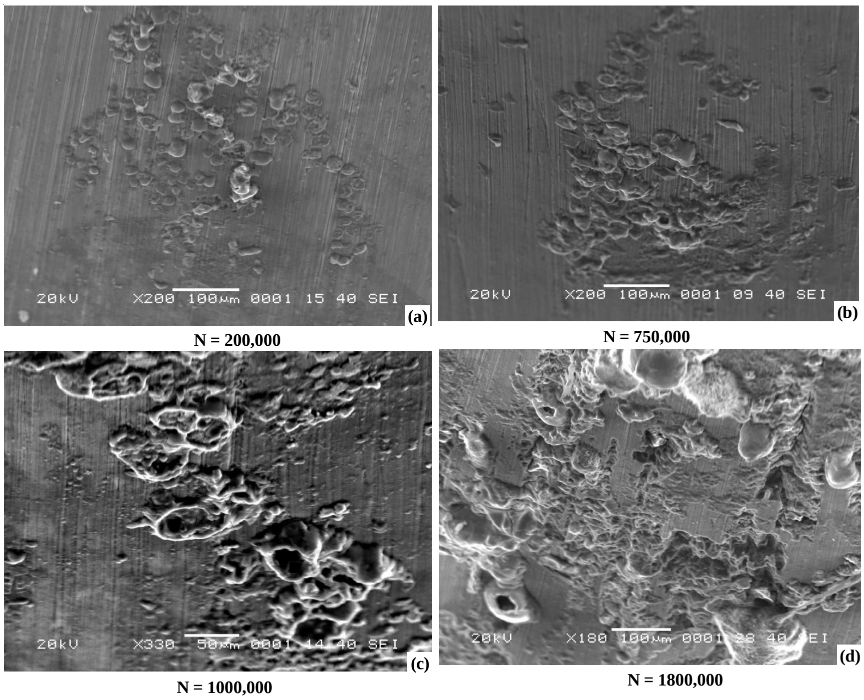

Figure 8. Specimen surface observations at the same location of the specimens tested under the NaCl environment at 50 MPa up to (a) 200,000 cycles, (b) 750,000 cycles, (c) 1000,000 cycles, and (d) 1800,000 cycles.

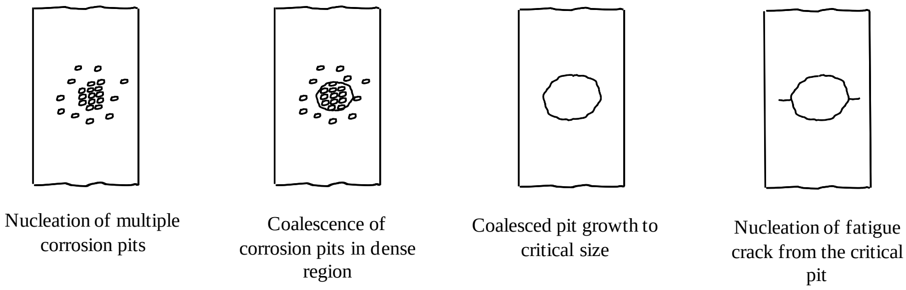

Figure 9. Schematic illustration showing the corrosion pit formation and growth of AZ31 alloy under the NaCl environment.

cence of corrosion pits in the localized area was found to form a large pit with further increase of cycles, as seen from Figure 8 (c) and 8 (d). This large coalesced pit could become a fatigue crack starter even at very low stress amplitude. A similar pit formation and growth mechanism has been observed for extruded AZ61 magnesium alloy at low stress amplitudes under the NaCl environments (Bhuiyan *et al.*, 2008).

Based on the experimental results, the pit formation process of the extruded AZ31 alloy under the NaCl environment at low stress amplitudes is schematically shown in Figure 9. The pit formation process and the fracture mechanism of the present material at low stress amplitude are suggested as follows:

1) Multiple corrosion pits nucleate in some localized area on the specimen surface.

2) Number of pits increases with increasing number of cycles.

3) Localized multiple dense pits coalesce to form a large pit.

4) Fatigue crack starts from the coalesced large pit when the pit size reaches to the critical size.

5) The fatigue crack grows to final failure.

Therefore, corrosion pit formation at low stress amplitudes under the NaCl environment will be the dominant factor for the reduced fatigue limit.

3.4 Relationship between stress amplitude and critical pit size

Mechanical stress is an important factor for the pit formation and growth under a corrosive environment (Bhuiyan *et al.*, 2008). Once a fatigue crack starts from the pit, stress around the pit is released and further pit growth is not significant. Therefore, it can be considered that the pit size observed at the fracture origin is the critical pit size for

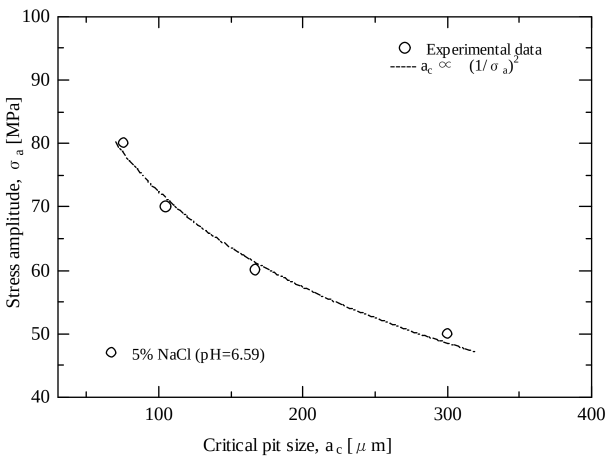

Figure 10. Variation of critical pit size with stress amplitude for AZ31 alloy under the NaCl environment.

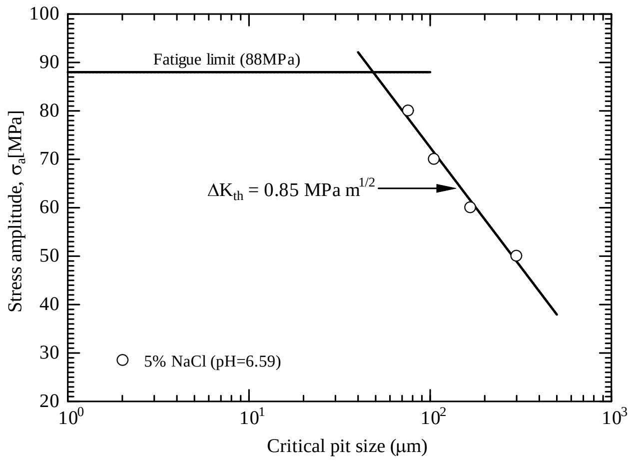

Figure 11. Critical pit size with stress amplitude for AZ31 alloy under the NaCl environment.

fatigue crack nucleation. The relationship between stress amplitude and critical crack size measured on fracture surface is shown in Figure 10. The pit size was defined as the radius of semi-circular crack (Dolley *et al.*, 2000; Bhuiyan *et al.*, 2008), which had the equivalent area to the pit observed at the crack nucleation site. Hoeppner (Hoeppner, 1978) has assumed that a fatigue crack nucleates from a corrosion pit when the pit grows to a critical size at which the stress intensity factor reaches the threshold value, by considering a corrosion pit as a surface crack. According to this assumption, the relationship between critical pit size and stress amplitude should follow the fracture mechanical relationship, $D_c \propto \left(1/\sigma_a \right)^2$. As can be seen from Figure 10, the experimental results are in good agreement with the fracture mechanical relationship, where a proportionality constant of the fracture mechanical relationship has been adjusted to give a good fit.

Figure 11 shows the relationship between stress amplitude and critical pit size under the NaCl environment in the form of the Kitagawa-Takahashi Diagram (Kitagawa *et al.*, 1976). As can be seen from the figure, the relationship under the NaCl environment is almost a straight line for all stress amplitudes tested. The straight line gives the threshold stress intensity factor range as 0.85 $MPa\sqrt{m}$. Therefore, this linear relationship suggests that a fatigue crack starts from a pit when the stress intensity factor range reaches the threshold value of 0.85. The value of 0.85 is similar to those obtained in the previous works: 0.8 for AZ61 under NaCl and $CaCl_2$ environment (Bhuiyan *et al.*, 2008), 0.64 for AM60 under 5% NaCl environment (Khan, 2007), respectively.

4. Conclusions

Fatigue tests were carried out under two corrosive environments and also in air to understand the basic corrosion fatigue behavior of extruded AZ31 magnesium alloy. From the results obtained, the following conclusions can be drawn.

1. A two-stage S-N curve was found under corrosive environments for AZ31, which would result from the difference in the crack nucleation mechanism between the stress levels above and below the fatigue limit under non-corrosive environment.

2. The fatigue limit under low humidity (36-40% relative humidity) without influence of corrosion was obtained as 88 MPa.

3. The fatigue strength at 10^7 cycles was reduced to 75 MPa under high humidity (80%RH). The reduction rate of fatigue limit (RRFL) due to high humidity was 15%, which indicates that the fatigue strength of AZ31 magnesium alloy is sensitive to the humidity level of ambient environment.

4. The fatigue strength at 10^7 cycles under the NaCl environment was 40 MPa. The RRFL value under the NaCl environment was 55%.

5. The drastic reduction in fatigue strength under corrosive environments resulted from pit formation and growth to the critical size for fatigue crack nucleation. It was found that at low stress amplitudes under corrosive environments multiple corrosion pits nucleated on the specimen surface, grew and then coalesced to form a large corrosion pit.

Acknowledgement

The authors deeply thank Mr. Murai and Mr. Iwakami from Sankyo Tateyama Aluminum Inc., Takaoka, Japan, for their cooperation and help.

References

Asami, K. and Sugiyama, Y. 1985. Fatigue strength of various surface hardened steels. Journal of Heat Treatment Technology 25(3), 147-150.

Ambat, R. Aung, N. N. and Zhou, W. 2000. Evaluation of microstructural effects on corrosion behavior of AZ91D magnesium alloy. Corrosion Science. 42(8), 1433-1455.

Arruebarrena, G.. Hurtado, I. and Bronfin, B. 2005. Weight reduction in Aircrafts by means of New Magnesium Castings. Journal of Materials Science and Technology. 13-20.

Abbas, G. Liu, Z. and Skeldon, P. 2005. Corrosion behaviour of laser-melted magnesium alloys, Applies Surface Science. 247 (1-4), 347-353.

Bayoumi, M. R. 1993. Fatigue behaviour of a commercial aluminium alloy in sea water at different tempers. Engineering Fracture Mechanics. 43(3), 297-307.

Bhuiyan, M.S. Mutoh, Y. Murai, T. and Iwakami, S. 2008. Corrosion Fatigue Behavior of Extruded Magnesium Alloy AZ61 under Three Different Corrosive Environments. International Journal of Fatigue. 30(10-11), 1756-1765.

Dieter, G. E. 1970. Mechanical Metallurgy, New York, McGraw Hill Co.

Davis, J. R. 1998. Corrosion-Understanding the basics, Ohio, ASM Intl Materials Park.

Dolley, E. J. Lee, B. and Wei, R.P. 2000. The effect of pitting corrosion on fatigue life. Fatigue & Fracture of Engineering Materials & Structure. 23, 555-560.

Euromech Colloquium 382, Fatigue & Fracture of Engineering Materials & Structure 1999; 22(7) and 22(8).

Forest, P. G. 1970. Fatigue of metals, Oxford, Pergamon..

Friedrich, H. and Schumann, S. 2001. Research for a “new age of magnesium” in the automotive industry. Journal of Materials Processing Technology. 117, 276-281.

Gough, H. J. 1932. Corrosion fatigue of metals. Journal of the Institute of Metals. 49,17-92.

Gray, J.E. and Laun, B. 2002. Protective coatings on magnesium and its alloys-a critical review. Journal of Alloys and Compounds, 88-113.

Hoeppner, D. W. 1978. Model for Prediction of Fatigue Lives Based Upon a Pitting Corrosion Fatigue Process, ASTM special Technical Publication (675), Symp on Fatigue Mech; Kansas city, MO, USA, 841-870.

Hilpert, M. and Wagner, L. 2000. Corrosion Fatigue Behavior of the High-Strength Magnesium Alloy AZ80. Journal of Materials Engineering and Performance. 9(4), 402-407.

Hilpert, M. and Wagner, L. 2000. Environmental Effects on the HCF Behavior of the Magnesium alloys AZ31 and AZ80, The Minerals, Metals and Materials Society. 375-381.

Kitagawa, H. and Takahashi, S. 1976. Applicability of fracture mechanics to very small cracks or the cracks in the early stages. In Proceedings of the Second International Conference on Mechanical Behavior of Materials, Metals Park, OH: American Society for Metals, 627-631.

Khan, S. A. 2007. Fatigue Behavior of Magnesium Alloys under Ambient and Corrosive Environments, Ph.D. thesis, Nagaoka University of Technology, 7-8.

Kulekci, M. K. 2008. Magnesium and its alloys applications in automotive industry. The International Journal of Advanced Manufacturing Technology. 39, 851-865.

Luo, A. A. 2002. Magnesium: Current and Potential Automotive Applications. JOM. 42-48.

McAdam, D. J. Jr. and Geil, G. W. 1941. Pitting and its effect on fatigue limit of steels corroded under various conditions. Proc Am Soc Testing Mater. 141, 696-701.

Magnin, T. Desijardins, D. and Puiggali, M. 1989. Influence of the mechanical test conditions on the corrosion fatigue behaviour of austenitic stainless steel in chloride solutions. Corrosion Science. 29 (5), 567-576.

Makar, G. L. and Kruger, J. 1990. Corrosion Studies of Rapidly Solidified Magnesium Alloys, Journal of the Electrochemical Society. 137 (2), 414-421.

Mordike, B. L. Ebert, T. 2001. Magnesium Properties-applications-potentioal. Materials Science and Engineering: A. 302, 37-45.

Pokhmurskii, V. I. 1983. General aspects of corrosion on fatigue in metals and alloys. Proceedings of the 1st-USSR-UK Seminar on Corrosion Fatigue of Metals, London, The Metal Society, 47-53.

Rosalbino, F. Angelini, E. Negri, S. D. Saccone, A. and Delfino, S. 2005. Effect of erbium addition on the corrosion behaviour of Mg-A1 alloys, Intermetallicas. 13 (1), 55-60.

Song, G. Atrens, A. and Dargusch, M. 1999. Influence of microstructure on the corrosion of diecast AZ91D. Corrosion Science. 41(2), 249-273.

Schijve, J. 2003. Fatigue structures and materials in the 20th century and the state of the art. International Journal of Fatigue. 25, 679-702.

Sajuri, Z. B. Miyashita, Y. and Mutoh, Y. 2005. Effect of humidity and temperature on the fatigue behavior of an extruded AZ61 magnesium alloy. Fatigue & Fracture of Engineering Materials & Structure. 28, 373-379.

Somekawa, H. Kim, H. S. Singh, A. and Mukai, T. 2007. Fracture toughness in direct extruded Mg-Al-Zn alloys. Journal of Materials Research. 22(9), 2598-2607.

Uhlig, H. H. Devereux, O. F. McEvily, A. J. and Teahle, R. W. 1971.Corrosion Fatigue National Association of Corrosion Engineers, (Eds.), NACE-2, Houston, TX, 270.

Unigovski, Y. Eliezer, A. Abramov, E. Snir, Y. and Gutman, E. M. 2003. Corrosion Fatigue of Extruded magnesium alloys. Materials Science and Engineering : A. 360, 132-139.

Wescott, B. B. 1938. Fatigue and corrosion fatigue of steels. Trans. American Society of Mechanical Engineering. 60, 813-829.